A unified input–output analysis of four-bar linkages

Shaoping Bai [a],*, Jorge Angeles [b]

[a] *Department of Mechanical Engineering, Aalborg University, 9220 Aalborg, Denmark*
[b] *Department of Mechanical Engineering and Centre for Intelligent Machines, McGill University, 817 Sherbrooke,*
St. W. Montreal, Canada H3A 2K6

Abstract

Proposed in this paper is a unified, robust algorithm for the input–output analysis of planar, spherical and spatial four-bar linkages. Robustness is needed to account for architecture and algebraic singularities that are likely to occur, for example, when conducting an iterative optimization of the linkage at hand. The unified feature of the algorithm is based on the algebra of dual numbers and the Principle of Transference, which allows the extension of the algorithm developed for spherical linkages to their spatial counterparts by a simple *dualization* of the *real* geometric relations derived for the former. Numerical examples are included to demonstrate the application of the algorithm.
© 2007 Elsevier Ltd. All rights reserved.

Keywords: Dual numbers; Four-bar linkages; The Principle of Transference; Robust input–output analysis

1. Introduction

In designing spatial mechanisms, a robust algorithm of input–output analysis of four-bar linkages is desirable in order to account for architecture and algebraic singularities. For planar, spherical, and spatial four-bar linkages, their displacement analysis has been extensively studied and reported in the technical literature [1–10]. Generally, the analysis of four-bar linkages boils down to solving a system of trigonometric equations. The established approach to solving this system relies on transforming the equations at hand into polynomial equations by means of the trigonometric tan-half-angle identities. However, this transformation entails a singularity at π, i.e., when one of the polynomial roots of the transformed equation becomes unbounded, which shows that this approach lacks robustness. To cope with this problem, we introduce a robust *geometric* approach to obtain the roots of the input–output (I/O) equation of four-bar linkages of the RCCC type, that is derived from the analysis of planar and spherical RRRR linkages.

The most straightforward way to derive the input–output equation of a spatial RCCC four-bar linkage is to apply the *Principle of Transference* [11–13]. The beginnings of this principle are traced back to the early 1960s.

---

* Corresponding author.
   E-mail addresses: shb@ime.aau.dk (S. Bai), angeles@cim.mcgill.ca (J. Angeles).

One of its most notable applications was reported by Yang and Freudenstein [14], who analyzed a RCCC spatial mechanism by *dualizing* the closure equations of a spherical four-bar mechanism.

Reported in this paper is a unified algorithm that, starting from the I/O equation of the spherical four-bar linkage, avoids the tan-half-angle singularity mentioned above. This is done by transforming the trigonometric equation into a geometric problem, namely, the location of the intersections of a line with the unit circle centered at the origin of the planar coordinate frame containing the line. Now let us recall that the solution of *any* quadratic equation is geometrically equivalent to finding the intersections of an *arbitrary* conic with a line. It should become apparent that reducing the problem at hand to finding the intersections of a circle with a line is a better-structured problem than the former, and hence, more robust. Given that the I/O analysis of planar and spherical four-bar linkages are formally identical, the analysis of the former is included for completeness. We tested our algorithm with the numerical example included in [14], which Yang and Freudenstein solved using an iterative method applied to a system of six non-linear equations in six unknowns. While the results obtained with the two distinct procedures match quite satisfactorily, our approach is based on a reduced system of three simpler equations, one linear and two quadratic.

The motivation behind the algorithm is the need to design robust overconstrained parallel-kinematics machines with *reduced mobility*, i.e., with motion capabilities lying within a proper subset of the group of rigid-body displacements [15]. Applications of the algorithm to the robust design of spatial mechanisms such as three-degree-of-freedom spherical wrists, accounting for revolute-axis misalignments, are possible with the formulation proposed here.

2. A robust analysis of planar and spherical four-bar linkages

The analysis proposed here for spatial four-bar linkages, also known as RCCC linkages, is based on robust algorithms for planar and spherical RRRR linkages, which we include here for completeness. By virtue of the broad common ground shared by planar and spherical four-bar linkages, we treat here their I/O analysis within the same framework.

2.1. I/O equations of RRRR linkages

A general planar four-bar linkage is shown in Fig. 1a, wherein the input and output angles are denoted by ψ and ϕ, respectively. The link lengths are defined by the set of parameters $\{a_i\}_1^4$. Moreover, the general I/O equation of the planar linkage of Fig. 1a can be written in the non-dimensional form [16]:

$$k_1 + k_2 \cos \phi - k_3 \cos \psi - \cos \psi \cos \phi - \sin \psi \sin \phi = 0 \tag{1a}$$

which is called the *Freudenstein equation*, with $\{k_i\}_1^3$ referred to as the *Freudenstein parameters*, and defined as

$$k_1 \equiv \frac{a_1^2 + a_2^2 - a_3^2 + a_4^2}{2a_2a_4}, \quad k_2 \equiv \frac{a_1}{a_2}, \quad k_3 \equiv \frac{a_1}{a_4} \tag{1b}$$
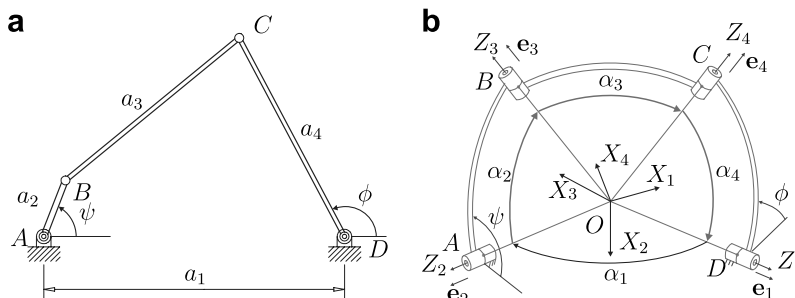

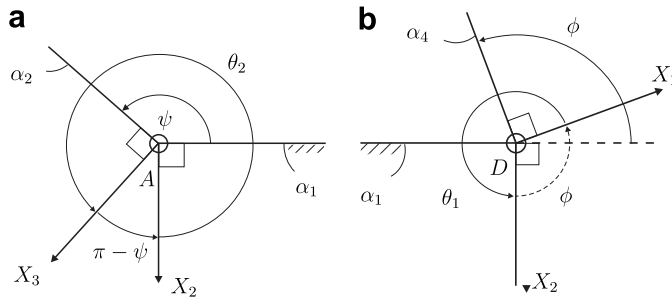Fig. 1. Four-bar linkages: (a) planar; and (b) spherical.

Fig. 2. Relations between input and output angles and those of the DH notation: (a) ψ and θ_2; and (b) ϕ and θ_1.

Depicted in Fig. 1b is the spherical counterpart of the foregoing four-bar linkage, made up of four revolute joints of axes intersecting at one common point O, the center of the linkage. The Denavit–Hartenberg (DH) notation [17] is adopted to define the linkage parameters and joint variables. Within this notation, the relation between ψ and θ_2 as well as that between ϕ and θ_1 is depicted in Fig. 2a and b, respectively.[1] Hence,

$$\psi = \theta_2 + \pi, \quad \phi = -\theta_1 \tag{2}$$

the latter following because $\phi + \theta_1 = 2\pi$ or 0.

The I/O equation of the spherical four-bar linkage takes the form [14]:

$$k_1 + k_2 \cos \psi + k_3 \cos \psi \cos \phi - k_4 \cos \phi + k_5 \sin \psi \sin \phi = 0 \tag{3a}$$

where

$$k_1 \equiv c\alpha_1 c\alpha_2 c\alpha_4 - c\alpha_3, \quad k_2 \equiv s\alpha_1 s\alpha_2 c\alpha_4, \quad k_3 \equiv c\alpha_1 s\alpha_2 s\alpha_4, \tag{3b}$$
$$k_4 \equiv s\alpha_1 c\alpha_2 s\alpha_4, \quad k_5 \equiv s\alpha_2 s\alpha_4 \tag{3c}$$

with $c(\cdot) \equiv \cos(\cdot)$, $s(\cdot) \equiv \sin(\cdot)$, and $\{\alpha_i\}_1^4$ denoting the linkage dimensions, as shown in Fig. 1b.

In observing the I/O equations of both the planar and spherical linkages, we notice that they both can be cast in the general form

$$A(\psi) \cos \phi + B(\psi) \sin \phi + C(\psi) = 0 \tag{4}$$

with the coefficients $A(\psi)$, $B(\psi)$ and $C(\psi)$ summarized in Table 1.

The solution of Eq. (4) for ϕ has been based on one of two distinct approaches, either purely numerical, by means of an iterative procedure [18,19], or algebraic, by means of a transformation of the trigonometric equation into an algebraic equation; the latter is done by means of the tan-half-angle identities:

$$\tan\left(\frac{\phi}{2}\right) \equiv \tau, \quad \sin \phi \equiv \frac{2\tau}{1 + \tau^2}, \quad \cos \phi \equiv \frac{1 - \tau^2}{1 + \tau^2} \tag{5}$$

Upon substitution of the foregoing identities into Eq. (4), a quadratic equation in τ is obtained:

$$D(\psi)\tau^2 + 2E(\psi)\tau + F(\psi) = 0 \tag{6}$$

whose corresponding coefficients $D(\psi)$, $E(\psi)$ and $F(\psi)$ are given in Table 2.

Now, ϕ can be readily computed once the two roots of Eq. (6) are available. Observing Eq. (6), one may realize that the roots can be found by simply applying the well-known formula for the roots of the quadratic equation. However, the said formula must be handled with care when finding its roots numerically. As Forsythe [20] pointed out, it is difficult to devise an algorithm that will safely solve the quadratic equation without the effect of round-off error amplification, as arising from what is called in numerical analysis *catastrophic can-*

---

[1] The lines labeled α_2 and α_4 in these figures are the front views of the planes defined by the axes Z_2 and Z_3, on which α_2 is measured, and by the axes Z_4 and Z_1, on which α_4 is measured, respectively.

Table 1
Coefficients of the trigonometric I/O equation

Case	$A(\psi)$	$B(\psi)$	$C(\psi)$
Planar	$k_2 - \cos\psi$	$-\sin\psi$	$k_1 - k_3\cos\psi$
Spherical	$k_3\cos\psi - k_4$	$k_5\sin\psi$	$k_1 + k_2\cos\psi$

Table 2
Coefficients of the polynomial I/O equation

Case	$D(\psi)$	$E(\psi)$	$F(\psi)$
Planar	$k_1 - k_2 + (1 - k_3)\cos\psi$	$-\sin\psi$	$k_1 + k_2 - (1 + k_3)\cos\psi$
Spherical	$k_1 + (k_2 - k_3)\cos\psi + k_4$	$k_5\sin\psi$	$k_1 + (k_2 + k_3)\cos\psi - k_4$

cellation. Moreover, the quadratic equation deflates for a value of $\phi = \pm\pi$; the deflated equation will produce only one solution in this case when, in fact, there actually exist two.

It is apparent that the quadratic-equation approach to the input–output analysis of the four-bar linkage would better be avoided, especially when writing code to implement this analysis. As an alternative, we can pursue a robust geometric approach, free of the *singularity* $\tau \to \pm\infty$ of the transformation of Eq. (5), as described in the balance of this section.

2.2. A geometric approach

Upon recalling Eq. (4) and rewriting it in a slightly different form, we obtain

$$\mathscr{L}: \quad A(\psi)u + B(\psi)v + C(\psi) = 0 \tag{7a}$$

where

$$u \equiv \cos\phi, \quad v \equiv \sin\phi \tag{7b}$$

and hence, u and v are subject to the constraint

$$\mathscr{C}: \quad u^2 + v^2 = 1 \tag{7c}$$

The input–output equation thus defines a line $\mathscr{L}$ in the u–v plane, while the constraint (7c) defines a unit circle $\mathscr{C}$ centered at the origin of the same plane. The circle is fixed, but the location of the line in the said plane depends on both the linkage parameters and the input angle ψ. Fig. 3 depicts the case of two distinct intersection points, where $\mathscr{N}$ is the normal to $\mathscr{L}$ passing through the origin.
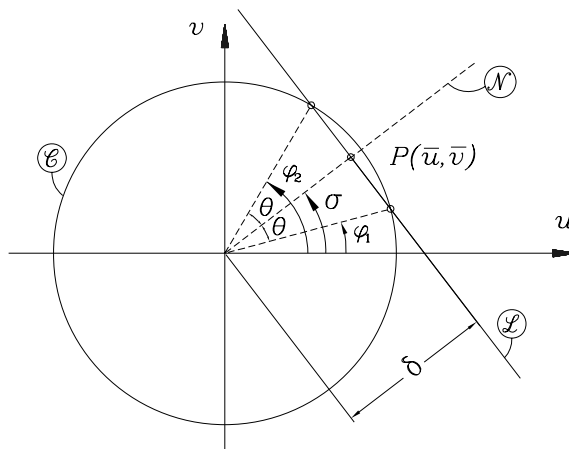

Fig. 3. Line and circle in the *u*–*v* plane.

Let the distance of the line to the origin be denoted by δ. Apparently, we have the three cases below:

(1) $0 < \delta < 1$: $\mathscr{L}$ intersects $\mathscr{C}$ at two distinct points, which correspond to two real and distinct solutions of ϕ for two *conjugate* postures of the linkage;
(2) $\delta = 1$: $\mathscr{L}$ is tangent to $\mathscr{C}$, indicating two real and identical solutions of ϕ, which means an extreme position of the output link; and
(3) $\delta > 1$: $\mathscr{L}$ does not intersect $\mathscr{C}$, implying that the input link is a rocker, the prescribed value of ψ lying outside the motion capabilities of this link.

The distance δ can be readily found to be

$$\delta = \frac{|C|}{\sqrt{A^2 + B^2}} \equiv \frac{|C|}{S} \tag{8}$$

whence, in the planar case—recalling the expressions of A and B from Table 1—the denominator S of Eq. (8) vanishes if and only if

$$\psi = 0 \quad \text{and} \quad k_2 = \frac{a_1}{a_2} = 1$$

and hence, $a_1 = a_2$, which is a pathological case, meaning that the input and the fixed links are of identical length and coincident. Moreover, for the quadrilateron to fold—$\psi = 0$—under these conditions, we must satisfy the condition, $a_3 = a_4$, which then leads to the equality, $k_1 = k_3$. Under these conditions, the numerator of Eq. (8) would also vanish, i.e.,

$$C(\psi; k_1, k_3) = k_1 - k_3 \cos \psi = k_1(1 - \cos \psi) = 0$$

Hence, the condition, $S = 0$ in Eq. (8) leads to $C = 0$, which in turn leads to δ being indeterminate. By the same token, for the spherical case, the indeterminacy of δ occurs when

$$\psi = 0 \quad \text{and} \quad k_3 = k_4$$

which implies that either $\alpha_2 = \alpha_1$ or $\alpha_2 = \alpha_1 + \pi$. By following a similar reasoning as in the planar case, we have either $\alpha_4 = \alpha_3$ or $\alpha_4 = \alpha_3 + \pi$, which leads to $k_1 = -k_2$. Correspondingly, the value of C is

$$C(\psi; k_1, k_2) = k_1 + k_2 \cos \psi = 0$$

Hence, for both the planar and spherical cases, if S vanishes, then C does as well, and the output angle becomes indeterminate. The geometric meaning of this case is that the output and the coupler links coincide as well, the four-bar linkage thus degenerating into an open two-link, spherical chain, and hence, *any* value of ϕ verifies the input–output equation. Notice that this pathological case is not apparent in the quadratic equation.

Moreover, in this particular case of δ-indeterminacy, when $A = B = C = 0$, the line $\mathscr{L}$ disappears for all values of the output ϕ, and we are left only with the circle, which means that ϕ is free to take any value.

Next, we turn to the general case of two intersections, i.e., with $0 < \delta < 1$. In order to compute the two conjugate values ϕ_1 and ϕ_2, we calculate first the intersection of $\mathscr{L}$ with its normal $\mathscr{N}$ from the origin. The intersection point has the coordinates $(\bar{u}, \bar{v})$ given below:

$$\bar{u} = -\frac{AC}{A^2 + B^2}, \quad \bar{v} = -\frac{BC}{A^2 + B^2} \tag{9}$$

whose denominator cannot possibly vanish, outside of the pathological case identified above. Now, the angle σ between $\mathscr{N}$ and the u axis, and the angle θ, defined as half the angle subtended by the chord defined by the intersections of $\mathscr{L}$ with $\mathscr{C}$, are given by

$$\sigma = \arctan\left(\frac{\bar{v}}{\bar{u}}\right), \quad \theta = \arccos(\delta) \tag{10}$$

and hence, the values of the two output angles are determined as

$$\phi_1 = \sigma - \theta, \quad \phi_2 = \sigma + \theta, \qquad \text{for } 0 < \delta < 1 \tag{11}$$

Notice that, for $\delta = 1$, $\theta = 0$ and the above equation yields $\phi_1 = \phi_2 = \sigma$. When $\delta = 0$, σ cannot be calculated from the above expression, but rather as $\arctan(-1/m)$, where m is the slope of $\mathscr{L}$. Nevertheless, in this case σ is not needed, for the two conjugate values of the output angle can be calculated directly. Indeed, for this case we have

$$\phi_1 = \arctan\left(\frac{-A}{B}\right), \quad \phi_2 = \phi_1 + \pi, \qquad \text{for } \delta = 0 \tag{12}$$

Finally, for the case $\delta > 1$, there is no real solution.

We have thus devised a general algorithm that can be applied to any planar or spherical four-bar linkage. The algorithm finds the intersections of the line $\mathscr{L}$ with the unit circle $\mathscr{C}$, as seen in Fig. 3, which in turn yields the two conjugate output angles ϕ_1 and ϕ_2 for a given input angle ψ.

3. A robust analysis of spatial four-bar linkages

The Principle of Transference will be used to devise a robust algorithm for the I/O analysis of the RCCC linkage. This principle states that the geometric relations of a spatial linkage can be derived by *dualizing* the counterpart relations for a spherical linkage.[2] In this process real numbers are substituted with *dual numbers*. Since the algebra of dual numbers is well documented in the literature [21], we will not dwell on the fundamentals here. The interested reader is directed to the foregoing reference. The algebra of dual numbers was summarized, its extension to dual vectors recalled, and an outline of its extension to dual matrices proposed in a tutorial paper [22], which includes examples illustrating the power of dual algebra in kinematics.

3.1. The I/O equation of the RCCC four-bar linkage

By means of the Principle of Transference, one can derive the input–output equation of the spatial four-bar linkage depicted in Fig. 4, where ψ and ϕ are included beside angles θ_1 and θ_2 of the DH notation. Angles ψ and ϕ are measured in exactly the same form as their counterparts in the planar and spherical cases. These angles follow the relationships of Eq. (2). By simply dualizing the counterpart spherical I/O equation (7a), we obtain

$$\widehat{A}\hat{u} + \widehat{B}\hat{v} + \widehat{C} = 0 \tag{13a}$$

where

$$\hat{u} = u - \epsilon d_4 v, \quad \hat{v} = v + \epsilon d_4 u, \quad u \equiv \cos\phi, \quad v \equiv \sin\phi \tag{13b}$$

with d_4 denoting the translation of the output cylindrical pair, while ϵ is the dual unit, which has the properties $\epsilon \neq 0$ and $\epsilon^2 = 0$. Moreover,

$$\widehat{A} = A + \epsilon A_0, \quad \widehat{B} = B + \epsilon B_0, \quad \widehat{C} = C + \epsilon C_0 \tag{13c}$$

whose primal parts A, B and C are identical to those of the spherical linkage, their dual parts A_0, B_0 and C_0 being obtained with the aid of computer algebra and the rules of operations with dual numbers, namely,

$$A_0 = a_{\max}(k_{30}c\psi - \lambda k_3 s\psi - k_{40}) \tag{14a}$$
$$B_0 = a_{\max}(k_{50}s\psi + \lambda k_5 c\psi) \tag{14b}$$
$$C_0 = a_{\max}(k_{10} + k_{20}c\psi - \lambda k_2 s\psi) \tag{14c}$$

in which the Freudenstein parameters are now dual numbers: $\hat{k}_i = k_i + \epsilon k_{i0}$, while λ is defined as the ratio

$$\lambda \equiv d_1/a_{\max} \tag{14d}$$

---

[2] Dualizing is sometimes referred to as "putting hats" on all the variables and parameters in the spherical-linkage equations.
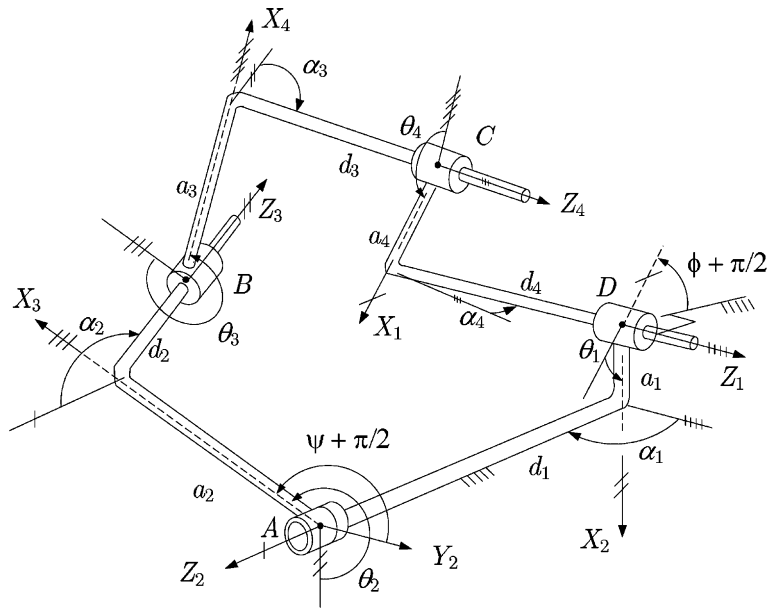
Fig. 4. Spatial RCCC linkage, described with the DH notation.

with[3] $a_{\max} = \max\{a_i\}_1^4$, and $r_i = a_i/a_{\max}$. Moreover,

$$k_{10} \equiv -r_1 s\alpha_1 c\alpha_2 c\alpha_4 - r_2 c\alpha_1 s\alpha_2 c\alpha_4 + r_3 s\alpha_3 - r_4 c\alpha_1 c\alpha_2 s\alpha_4 \tag{14e}$$

$$k_{20} \equiv r_1 c\alpha_1 s\alpha_2 c\alpha_4 + r_2 s\alpha_1 c\alpha_2 c\alpha_4 - r_4 s\alpha_1 s\alpha_2 s\alpha_4 \tag{14f}$$

$$k_{30} \equiv -r_1 s\alpha_1 s\alpha_2 s\alpha_4 + r_2 c\alpha_1 c\alpha_2 s\alpha_4 + r_4 c\alpha_1 s\alpha_2 c\alpha_4 \tag{14g}$$

$$k_{40} \equiv r_1 c\alpha_1 c\alpha_2 s\alpha_4 - r_2 s\alpha_1 s\alpha_2 s\alpha_4 + r_4 s\alpha_1 c\alpha_2 c\alpha_4 \tag{14h}$$

$$k_{50} \equiv r_2 c\alpha_2 s\alpha_4 + r_4 s\alpha_2 c\alpha_4 \tag{14i}$$

all being dimensionless. Once we have obtained the input–output equation in terms of dual angles, it is possible to analyze the RCCC linkage, which allows us, in turn, to compute all the joint rotations and translations. The input–output equation above can be generally written as

$$\widehat{\mathscr{L}}: \quad \widehat{A}\hat{u} + \widehat{B}\hat{v} + \widehat{C} = 0 \tag{15a}$$

and

$$\widehat{\mathscr{C}}: \quad \hat{u}^2 + \hat{v}^2 = 1 \tag{15b}$$

where

$$\hat{u} = \cos\hat{\phi}, \quad \hat{v} = \sin\hat{\phi} \tag{15c}$$

Eqs. (15a–c) represent a *dual line* $\widehat{\mathscr{L}}$ and a *dual unit circle* $\widehat{\mathscr{C}}$ in the dual $\hat{u}$–$\hat{v}$ plane, respectively. Now, it is possible to decompose the equation of the "line" $\widehat{\mathscr{L}}$ into two real equations, one for its primal, and one for its dual part, namely,

$$\mathscr{P}: \quad Au + Bv + C = 0 \tag{16a}$$

$$\mathscr{H}: \quad (A_0 + Bd_4)u + (B_0 - Ad_4)v + C_0 = 0 \tag{16b}$$

---

[3] Notice that, in the DH notation, parameters a_i are defined as *distances*, which, by definition, are non-negative. Hence, in the definition of $a_{\max}$, absolute values are obviated.

For the circle $\widehat{\mathscr{C}}$, the dual part vanishes identically, and we are left only with the primal part, namely,

$$\mathscr{C}: \quad u^2 + v^2 = 1 \tag{16c}$$

Eq. (16a) represents a plane $\mathscr{P}$ parallel to the d_4-axis in the (u, v, d_4)-space, while Eq. (16b) represents a hyperbolic paraboloid $\mathscr{H}$ in the same space. Moreover, Eq. (16c) represents a cylinder $\mathscr{C}$ of unit radius and axis parallel to the d_4-axis, all foregoing items being shown in Fig. 5a and b.

The three-dimensional geometric interpretation of Eqs. (16a–c) can be seen in Fig. 5a and b, whereby line $\mathscr{L}_i$, for $i = 1, 2$, is defined as the intersection of the plane of Eq. (16a) with the cylinder (16c). Moreover, each line $\mathscr{L}_i$ intersects the paraboloid (16b) at one single point, as illustrated in Fig. 5b, and as made apparent below.

The system of Eqs. (16a–c) should be solved for u, v and d_4 in order to calculate the two conjugate output angles and their corresponding output translations. The intersection points P_1 and P_2 thus yield the two conjugate output angles ϕ_1 and ϕ_2. Once the two conjugate solutions u and v are known, via the coordinates of P_1 and P_2, the unique value of d_4 corresponding to each solution, and defining the intersection points I_1 and I_2, is determined from Eq. (16b), namely,

$$d_4 = \frac{A_0 u + B_0 v + C_0}{Av - Bu}, \quad Av \neq Bu \tag{17}$$

Note that the denominator of Eq. (17) vanishes if $Av = Bu$; then, as can be readily verified, the numerator of d_4 in the above expression vanishes as well, and d_4 is indeterminate. In this case, the surface $\mathscr{H}$ disappears for all values of the output translations d_4 and we are left with the plane $\mathscr{P}$ and the cylinder $\mathscr{C}$, which means that d_4 is free to take any value. That is, the motion of this linkage in the plane normal to its joint axes is independent of the translations along these axes. We are here in the presence of a parametric singularity producing a degeneracy of the linkage, similar to those described for the planar and spherical linkages in Section 2. Under this singularity, all joint axes are parallel ($\alpha_i = 0, i = 1, \ldots, 4$) and, hence, the coupler and the output links can freely slide along their cylindrical-joint axes.

3.2. Canonical equation of the hyperbolic paraboloid $\mathscr{H}$

In order to gain insight into the problem geometry, we derive below the canonical equation of $\mathscr{H}$. To this end, we let

$$\mathbf{x} \equiv [u \quad v \quad d_4]^{\mathrm{T}}, \quad Q(\mathbf{x}) \equiv A_0 u + B d_4 u + B_0 v - A d_4 v + C_0$$

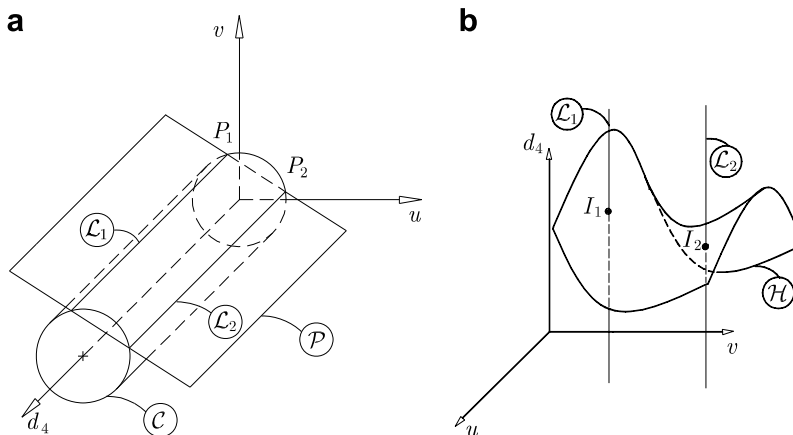the Hessian matrix $\mathbf{H}$ of $Q(\mathbf{x})$ then being evaluated as

Fig. 5. Intersections of (a) $\mathscr{P}$ and $\mathscr{C}$; and (b) $\mathscr{L}_i$ and $\mathscr{H}$, for $i = 1, 2$.

$$\mathbf{H} \equiv \frac{\partial^2 Q}{\partial \mathbf{x}^2} = \begin{bmatrix} 0 & 0 & B \\ 0 & 0 & -A \\ B & -A & 0 \end{bmatrix}$$

whose eigenvalues are readily computed as

$$\lambda_1 = -\sqrt{A^2 + B^2}, \quad \lambda_2 = 0, \quad \lambda_3 = \sqrt{A^2 + B^2}$$

The corresponding non-normalized eigenvectors $\mathbf{e}_i$, for $i = 1, 2, 3$, are

$$\mathbf{e}_1 = \begin{bmatrix} B \\ -A \\ \sqrt{A^2 + B^2} \end{bmatrix}, \quad \mathbf{e}_2 = \begin{bmatrix} A \\ B \\ 0 \end{bmatrix}, \quad \mathbf{e}_3 = \begin{bmatrix} -B \\ A \\ \sqrt{A^2 + B^2} \end{bmatrix}$$

and hence, the canonical equation of the surface $\mathscr{H}$ is of the form:

$$\zeta = \frac{\xi^2}{K} - \frac{\eta^2}{K}, \quad K = \frac{2(A_0 A + B_0 B)}{A^2 + B^2}$$

where

$$\xi = \frac{-\sqrt{2}}{2\sqrt{A^2 + B^2}} \left[Bu + Av + d_4 + \frac{A_0 B - B_0 A}{4(A_0 A + B_0 B)} \right]$$

$$\eta = \frac{\sqrt{2}}{4\sqrt{A^2 + B^2}} \left(Bu - Av + d_4 + \frac{A_0 B - B_0 A}{A_0 A + B_0 B} \right)$$

$$\zeta = \frac{1}{\sqrt{A^2 + B^2}} \left[Au + Bv + \frac{(A^2 + B^2) C_0 A}{A_0 A + B_0 B} \right]$$

which proves that $\mathscr{H}$ is indeed a hyperbolic paraboloid.

3.3. The case of d_4 acting as input

The motivation behind the algorithm reported here being the need for accommodating manufacturing and assembly errors in spatial mechanisms [23] and further, in parallel robots with reduced mobility, we include a case that has been overlooked in the literature. This case pertains to regarding the translational displacement of the output C joint of a RCCC linkage as input, the two outputs being angles ψ and ϕ. In this case the problem no longer leads to a quadratic equation, but rather to a system of one quartic and one quadratic equations in two variables, as described presently.

Eqs. (16a) and (16b) are both linear in u and v, which allows us to solve for these variables in terms of d_4, namely,

$$u = u(p, q) = \frac{-BC_0 + CB_0 - CAd_4}{-AB_0 + BA_0 + B^2 d_4 + A^2 d_4} \tag{18a}$$

$$v = v(p, q) = \frac{-CA_0 - AC_0 + CBd_4}{-AB_0 + BA_0 + B^2 d_4 + A^2 d_4} \tag{18b}$$

where, in light of Eq. (17), d_4 is an explicit function of u and v. Moreover, by virtue of Eqs. (14a–c), with $p = \cos \psi$ and $q = \sin \psi$, u and v become functions of p and q. The latter, additionally, are subject to

$$p^2 + q^2 = 1 \tag{19}$$

Substituting the values of u and v given above into Eq. (16c) produces an equation free of u and v or, correspondingly, free of ϕ, namely,

$$f(p, q) = 0 \tag{20}$$

From Table 1 and Eqs. (14a–c), both u and v are rational functions with both numerator and denominator quadratic in p and q. Hence, u^2 and v^2 are rational functions with both numerator and denominator quartic in p and q. Therefore, $f(p, q) = 0$ leads, after clearing denominators, to a quartic equation in p and q.

The system of polynomial equations (19) and (20) apparently has a Bezout number of $4 \times 2 = 8$.

4. Numerical examples

The proposed algorithm is validated with two numerical examples. All numerical and symbolic calculations were completed with the aid of Maple 9.0.

4.1. Example 1: The Yang and Freudenstein linkage

The first example is taken from [14], with data as listed in Table 3. The output displacements vs. the input angle are recorded in Table 4. For conciseness, we list only the results for $0 \leqslant \psi \leqslant \pi$. Our results match those reported in [14], considering the difference of input and output angles in both works, as explained is Section 2. Moreover, it is noteworthy that only two displacement equations need be solved in our method, as compared with the system of six equations in six unknowns formulated in [14], within a purely numerical approach. The

Table 3
DH parameters of a RCCC mechanism

Link	1	2	3	4
a_i (in.)	5	2	4	3
α_i (deg)	60	30	55	45
d_i (in.)	0	Variable	Variable	Variable

Table 4
RCCC displacements

ψ (deg)	ϕ (deg)	d_4 (in.)[a]	d_4 (in.)[b]
Branch 1			
0.0	83.7001529991332	−0.1731633276638529	−0.1731633276638444
20.0	68.5965846156616	0.01107737788443084	0.01107737788442875
40.0	64.21379652207564	−0.5291731035884291	−0.5291731035884372
60.0	67.55907288995121	−1.262205014939956	−1.262205014939955
80.0	75.72376607918567	−1.888758473657802	−1.888758473657801
100.0	87.21970036189694	−2.259417486910091	−2.259417486910097
120.0	101.1949771633546	−2.248309754267407	−2.248309754267406
140.0	116.6745933883008	−1.770565940896936	−1.770565940896947
160.0	131.8997403705473	−0.9205435136540786	−0.9205435136540738
180.0	144.2093802647503	−0.1150813700871400	−0.1150813700871402
Branch 2			
0.0	276.2998470008668	0.1731633276638416	0.1731633276638416
20.0	254.6701689686606	0.8429100434711766	0.8429100434711502
40.0	235.9479008729766	1.085719205870591	1.085719205870590
60.0	223.0109192021524	0.9378806906156329	0.9378806906156329
80.0	214.5328380596393	0.6631677056813780	0.6631677056813573
100.0	209.1315343183799	0.3676536168092682	0.3676536168092751
120.0	206.1460158532756	0.08437532803790148	0.08437532803790330
140.0	205.6297490641858	−0.1502382490993213	−0.1502382490993197
160.0	208.4003706539843	−0.2203697116995341	−0.2203697116995387
180.0	215.7906197352497	0.1150813700871401	0.1150813700871377

[a] From the proposed algorithm.
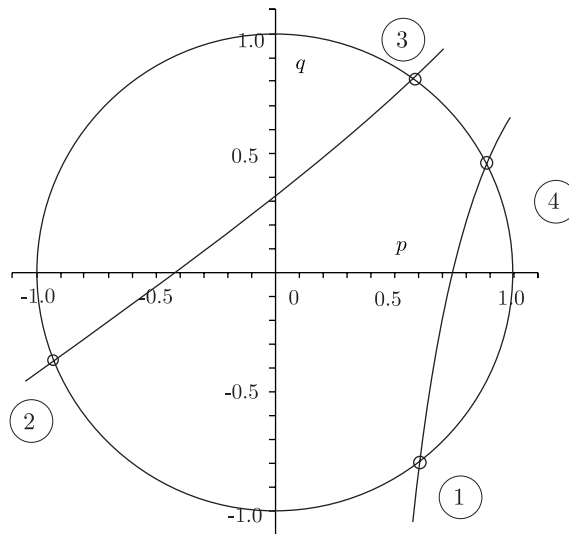[b] From Yang and Freudenstein's algorithm.

Fig. 6. The case of an input translation.

Table 5
Possible values of ψ and ϕ

	$[p, q]$	ψ (deg)	ϕ (deg)
1	[0.6047587377, −0.7964087325]	−52.78	[−65.68, −227.07]
2	[−0.9289796338, −0.3701308418]	−158.27	[−130.66, −207.99]
3	[0.5819053587, 0.8132565115]	54.41	[66.04, 226.10]
4	[0.8869350365, 0.4618941881]	27.50	[65.79, −113.02]

matching of the numerical values obtained with the two different methods is remarkable, with differences appearing only beyond the 10th digit.

4.2. Example 2: Prescribing d_4 as input

In the second example, we find the rotations ψ and ϕ for a given d_4 and given dimensions of a RCCC linkage. The dimensions are the same as those in Example 1, with $d_4 = 1.0$. In this example, Eq. (20) takes the form:

$$A_0 p^4 + A_1(q)p^3 + A_2(q)p^2 + A_3(q)p + A_4(q) = 0 \tag{21}$$

where coefficients $A_i(q)$, for $i = 0, \ldots, 4$, are given below:

$$A_0 = 0.09209746694$$
$$A_1(q) = -0.06765823468q - 0.0073324502$$
$$A_2(q) = -0.1754806581q^2 + 0.01487658368q - 0.1902460942$$
$$A_3(q) = 0.1353164694q^3 + 0.1202907568q^2 + 0.2424947249q + 0.04203177757$$
$$A_4(q) = -0.015625q^4 - 0.0811898817q^3 - 0.020697377q^2 - 0.1362382267q + 0.0484753242$$

Eq. (21) represents a curve in the p–q plane, whose intersections with the circle of Eq. (18) yield all real roots of the system at hand. Note, moreover, that all such roots are bound to lie on the above circle. The four real solutions of the foregoing system are given by the four intersections depicted in Fig. 6. The solutions are listed in Table 5, including the corresponding angles of rotation.[4]

---

[4] In this table only p and q are given with 10 digits; all other values are given with only four, for the sake of economy of space.

5. Conclusions

A robust geometric approach was proposed for solving the input–output equations of planar, spherical and spatial four-bar linkages. Within this approach, the well-known singularity-prone tan-half-angle transformation is avoided. This is done by resorting to a geometric representation of the I/O equation of the planar and spherical four-bar linkages, which leads to the problem of finding the intersection of a line and a unit circle whose plane contains the line. The dual counterpart of this representation leads to finding the intersections of three surfaces, a circular cylinder of unit radius, a plane parallel to the axis of the cylinder, and a hyperbolic paraboloid. The I/O analysis problem associated with RCCC linkages in which the displacement of the output translation plays the role of input was also included. We showed that the problem of determining angles ψ and ϕ, in this case, leads to the intersection of a quartic with a circle. An application of the algorithm reported here to the robust design of a parallel spherical wrist is to be reported in a forthcoming paper. In that design, the unactuated revolute joints are replaced by their cylindrical counterparts, each leg thus becoming a RCCC linkage.

Acknowledgments

References

[1] R. Beyer, Kinematische Getriebesynthese, Springer Verlag, Berlin–Göttingen–Heidelberg, 1953.
[2] C.H. Suh, C.W. Radcliffe, Kinematics and Mechanisms Design, Wiley, New York, 1978.
[3] K. Luck, K.H. Modler, Getriebetechnik—Analyse, Synthese, Optimierung, Springer-Verlag, Berlin, 1995.
[4] C.D. Crane III, J. Duffy, Kinematic Analysis of Robot Manipulators, Cambridge University Press, Cambridge, England, 1998.
[5] J.M. McCarthy, Geometric Design of Linkages, Springer-Verlag, New York, 2000.
[6] R.V. Dukkipati, Spatial Mechanisms: Analysis and Synthesis, Narosa Publishing House, 2001.
[7] R. Kreutzinger, Über die Bewegung des Schwerpunktes beim Kurbelgetriebe, Maschinenbau, Beilage Getriebetechnik 10 (1942) 397–398.
[8] K.-H. Sieker, Zur algebraischen Maßsynthese ebener Kurbelgetriebe, Archive of Applied Mechanics (Ingenieur Archiv) 24 (3) (1956) 188–215.
[9] E.E. Peisach, Analysis of link positions and domains of existence of the spatial RCCC mechanism. Part 1: Theory of mechanisms and machines, A Scientific Electronic Journal of St. Peterburg State Polytechnic University 1 (2) (2003) 17–27.
[10] E.E. Peisach, Analysis of link positions and domains of existence of the spatial RCCC mechanism. Part 2: Theory of mechanisms and machines, A Scientific Electronic Journal of St. Peterburg State Polytechnic University 2 (1) (2004) 2–25.
[11] F. Dimentberg, The screw calculus and its applications in mechanics, Izdat, Nauka, Moscow, English Translation: AD680993, Clearinghouse for Federal and Scientific Technical Information, 1965.
[12] O. Bottema, B. Roth, Theoretical Kinematics, Dover Publications, Mineola, NY, 1990.
[13] J. Rico Martínez, J. Duffy, The principle of transference: history, statement and proof, Mechanism and Machine Theory 28 (1993) 165–177.
[14] A. Yang, F. Freudenstein, Application of dual-number quaternion algebra to the analysis of spatial mechanisms, Journal of Applied Mechanics 31 (1964) 300–307.
[15] J. Angeles, The degree of freedom of parallel robots: a group-theoretic approach, in: IEEE International Conference on Robotics and Automation, Barcelona, 2005, pp. 1017–1024.
[16] F. Freudenstein, Approximate synthesis of four-bar linkages, Transactions of the ASME 77 (1955) 853–861.
[17] J. Denavit, R. Hartenberg, Kinematic Synthesis of Linkage, McGraw Hill Book Company, New York, 1964.
[18] H. Kerle, R. Pittschellis, Einführung in die Getriebelehre, second ed., B.G. Teubner GmbH, Stuttgart–Leipzig–Wiesbaden, 2002.
[19] VDI, Richtlinie VDI2729, Modulare kinematische Analyse ebener Gelenkgetriebe mit Dreh- und Schubgelenken, VDI, Düsseldorf, 1995.
[20] G.E. Forsythe, Pitfalls in computation, or why a math book isn't enough, American Mathematical Monthly 77 (1970) 931–956.
[21] I. Fischer, Dual Number Methods in Kinematics, Statics and Dynamics, CRC Press, New York, 1999.
[22] J. Angeles, Application of dual algebra to kinematic analysis, in: J. Angeles, E. Zakhariev (Eds.), Computational Methods in Mechanical Systems, NATO ASI Series, Springer-Verlag, New York, 1998.
[23] F. Bidault, C.P. Teng, J. Angeles, Structural optimization of a spherical parallel manipulator using a two-level approach, in: Proceedings of ASME 2001 Design Engineering Technical Conferences, DAC-21030, 2001.